

Received September 25, 2019, accepted November 15, 2019, date of publication November 25, 2019, date of current version December 10, 2019.

Digital Object Identifier 10.1109/ACCESS.2019.2955715

A Comparison Between Measured and Computed Assessments of the RF Exposure Compliance Boundary of an In-Situ Radio Base Station Massive MIMO Antenna

ROB WERNER¹, PHILL KNIPE^{2,5}, AND STEVE ISKRA^{3,4,5}

¹ Singtel Optus Pty Limited, Cannon Hill, QLD 4170, Australia

² Total Radiation Solutions, Claremont, WA 6010, Australia

³ Telstra Corporation Ltd., Melbourne, VIC 3000, Australia

⁴ Swinburne University of Technology, Hawthorn, VIC 3122, Australia

⁵ Australian Centre for Electromagnetic Bioeffects Research (ACEBR), Wollongong, NSW 2522, Australia

Corresponding author: Rob Werner (rob.werner@optus.com.au)

ABSTRACT Advanced antenna technology in the form of massive multiple input multiple output (mMIMO) antennas has been deployed in fourth generation (4G) long term evolution (LTE) mobile networks and will be a standard feature in fifth generation (5G) networks. A characteristic of mMIMO is beamforming in which a large array of antenna elements is used to concentrate energy in specific narrow directions to improve data throughput. Assessing the electromagnetic field (EMF) compliance boundary around a beamforming capable mMIMO antenna using a traditional approach that assumes maximum power is simultaneously transmitted in every possible direction and the radio base station (RBS) is fully loaded (100% traffic utilization) may produce very conservative results. In this study we report on measurements of the 6-minute time-averaged EMF levels in front of a mMIMO antenna operating in a 4G LTE time division duplex (TDD) network and compare results with conservatively computed EMF levels. The RBS serves users scattered throughout a dense urban environment characterized by low rise commercial/industrial buildings. When scaled to 100% RBS traffic loading and taking TDD operation into account, the highest measured EMF level was 7.3% to 16.1% of the ICNIRP occupational reference level compared to a conservative computed level of 79.3%. This represents a far-field reduction in the occupational compliance boundary of between 2.2 and 3.3 times and is consistent with other statistically based theoretical studies. An additional reduction in the compliance boundary can be expected due to actual RBS traffic loading often being much less than 100%.


INDEX TERMS Mobile communication, EMF exposure, base stations, RF EMF compliance, massive MIMO, antenna arrays, beamforming.

I. INTRODUCTION

The determination of the compliance boundary around a mobile communications radio base station (RBS) antenna is often a regulatory requirement imposed by national or state authorities with the requirement that the time-averaged radiofrequency (RF) electromagnetic field (EMF) exposure outside the boundary shall not exceed the levels in EMF safety standards such as those published by ICNIRP [1] or IEEE [2]. Methods of assessing compliance boundaries have

been published in standards such as IEC 62232 [3] where measurement and computation are equally valid approaches.

In many cases a typical approach to the determination of an EMF compliance boundary is through computational modelling. Computations are based on static (unchanging) 120° sector antenna patterns and assume maximum transmitter power and constant 100% traffic loading to generate 'worst-case', conservative EMF compliance boundary. Interestingly, while this approach has been generally accepted to date for existing 2G, 3G and 4G mobile systems, information gathered about user traffic has found that actual RBS traffic loading in these network is very likely to be less than 100% [4], [5] so

The associate editor coordinating the review of this manuscript and approving it for publication was Haiwen Liu .

that in everyday situations the actual compliance boundary around existing RBS antennas will be smaller than that determined by the conservative approach.

Multiple input multiple output (MIMO) antenna technology has been in use for a number of years. It utilizes multiple antennas to improve the reliability of transmission by taking advantage of independent (uncorrelated) propagation paths (spatial diversity). More recently, massive MIMO (mMIMO) antenna technology has been developed utilizing a higher number of antenna elements (typically >64) that enables the dynamic combination of two additional concepts to increase capacity, spatial multiplexing and beamforming. Spatial multiplexing seeks to transmit independent data over multiple uncorrelated paths by taking advantage of scattering from multiple surfaces while beamforming enables the antenna to target specific users in smaller regions of space. In 5G networks, mMIMO is mainly applied at the RBS with user devices implementing basic beam forming schemes.

Compared to traditional sector RBS antennas ($\sim 120^\circ$ beam width, ~ 17 dBi gain), beamforming mMIMO antennas can generate relatively narrow high gain beams ($\ll 120^\circ$ beam width, up to ~ 24 dBi or more gain) to better target RF energy towards users to improve signal-to-noise ratio, minimize interference from adjacent users and improve overall channel traffic transmission performance. Furthermore, multiple user mMIMO technology can target more than one spatially separated user simultaneously by employing multiple beams thereby increasing traffic throughput and minimizing user delays. When serving multiple users simultaneously, the transmitter power is split across the different directions. A fundamental difference then between mMIMO and traditional sector antennas is that in real life situations, under actual traffic conditions, the radiation pattern of a mMIMO antenna is dynamic and constantly changing, not static. It adjusts in response to the demands of users distributed spatially across the cell and takes advantage of multiple uncorrelated propagation paths to deliver increased capacity through multiple parallel data streams [8], [9].

Determining the EMF compliance boundary around mMIMO antennas has become of interest as 5G networks begin to be deployed alongside existing mobile technologies. A traditional, conservative approach to determining the compliance boundary for a mMIMO antenna would assume that the radiated power was equivalent to the simultaneous transmission of all possible array beams where each beam is continuously transmitting at the theoretical maximum transmitter output power. It might also assume that the RBS is 100% loaded with user traffic and no account is taken of time-division duplex (TDD) operation.

Recent studies using statistical approaches to assess EMF levels from mMIMO antennas under real life conditions have found that time-averaged RF exposure will be well below levels determined using a traditional conservative approach [7]–[9]. The reduced time-averaged exposure is due not only to the ‘bursty’ nature of user traffic, but also to the intermittent, random like exposure to mMIMO beams. These

findings imply that compliance boundaries determined using traditional, conservative assumptions will be much larger than boundaries determined using realistic assumptions or actual information about the operation of RBSs under everyday situations.

In this study we report on a novel campaign involving measurements of the 6-minute (6-min) [1] time-averaged RF exposure using multiple EMF probes spatially distributed in front of a mMIMO antenna operating in a 4th generation (4G) long term evolution (LTE) time division duplex (TDD) network and compare results with conservative calculations of EMF levels at the same positions. Simultaneous measurements from multiple EMF probes provide insights into the spatial distribution over time of the radiated power from the mMIMO antenna that are unavailable when using a single probe. The purpose of this comparison is to determine the extent of overestimation, if any, in the size of a conservatively computed EMF compliance boundary when compared to a boundary based on measured EMF levels from a mMIMO antenna operating in a live network. We also compare our measurement results with those of theoretically based statistical studies that indicate in mMIMO networks, the intermittent, random like behavior of beamforming will reduce time-averaged RF exposure and lead to smaller compliance boundaries compared to those based on conservative assumptions of RBS activity.

II. METHOD

A. MEASUREMENT OVERVIEW

Measurements were performed on a RBS in a commercial/industrial site close to the central business district of Melbourne, Australia. The sector chosen for measurements was a dense urban environment with low rise buildings as shown in Fig. 1.



FIGURE 1. A mMIMO antenna facing a dense urban environment with low rise commercial/industrial buildings (photo taken from the viewpoint of the antenna).

The RBS was an Optus, 4G LTE site operating in time division duplex (TDD) mode (three downlink (DL) subframes to one uplink (UL) subframe, referred to as a TDD ratio of 0.75 (75% DL transmission time)) at 2.3 GHz utilizing beamforming mMIMO antennas that are capable of up to eight simultaneous beams. The antennas were located on a rooftop that provided convenient access with ample space for the setup of an array of seven measurement probes.

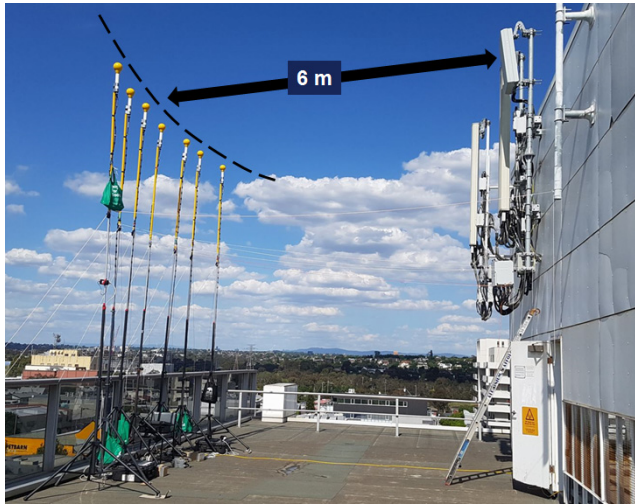


FIGURE 2. Measurement probes in front of the mMIMO antenna with 8° of mechanical down tilt. The middle probe is aligned with antenna boresight.

The probes were spaced in azimuth and positioned 6 m in front of the mMIMO antenna as shown in Fig. 2. The distance of 6 m was the maximum available separation on the rooftop and was close to the computed far field distance of 8 m from the antenna.

The mMIMO antenna contains 192 antenna sub elements arranged into 64 active elements in an 8x8 array and is capable of up to eight MIMO layers. Maximum gain occurs when the array is controlled to focus RBS power to a single point in the direction of boresight. This single beam has a gain of 23.6 dBi and width 9° in elevation and 14° in azimuth. The RBS has three 20 MHz TDD carriers (total bandwidth of 60 MHz) at 2.3 GHz each operating at 40 W for a total power into the antenna of 120 W (50.8 dBm) which equates to an effective isotropic radiated power (EIRP) of 74.4 dBm. When adjusted for TDD transmission (ratio 0.75) the maximum radiated power is $EIRP_{max} = 73.2$ dBm. The antenna has 8° of mechanical downtilt and is designed to cover a sector of ±60° in azimuth and ±20° in elevation. The gain of the beam reduces away from boresight and is 1.8 dB lower at ±40° in azimuth. When simultaneously serving multiple spatially separated users with n different beams, the EIRP of each beam is reduced equally to $EIRP_{max} - 10\log_{10}(n)$ ($1 \leq n \leq 8$).

Alignment and angular spacing of the measurement probes in two horizontal planes relative to the mMIMO antenna is shown in Fig. 3. The measurement planes were determined based on the topography of the coverage area to ensure that the probes would be in the path of beams serving mobile devices in the target sector. The combination of seven measurement probes and two measurement planes were chosen to maximize the likelihood of capturing the peak EMF level.

The higher positioned plane (Hi) cuts through boresight while the lower plane (Lo) is 6° below boresight. Plane Hi was aligned towards the cell boundary. Both the vertical (6°)

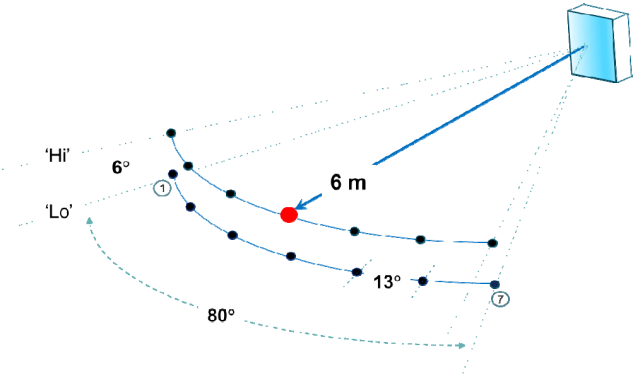


FIGURE 3. Schematic showing position of seven probes in two horizontal planes marked Hi and Lo in front of the mMIMO antenna. The nominal boresight probe position is marked by the larger red filled circle. All other probe locations are marked by dark filled circles. The probe positions in azimuth are numbered numerically from 1 to 7. For example, bore site is position 4Hi.

and horizontal (13°) spacing between probes was intended to approximately match the width of a single beam as described earlier. This allows the simultaneous detection of individual beams directed along seven azimuthal directions in a single plane. Individual sets of measurements were made for each plane. The total instantaneous EMF level at each probe will be a function of users in the sector served by a beam and side lobes from adjacent beams serving other users.

While the aim was to locate the probes in the far field (8 m) of the mMIMO antenna, roof space limitations meant that only a closer distance of 6 m was available. The EMF RF exposure level at this distance was computed using the software tool IXUS (IXUS EMF Compliance Management Software by Alphawave Pty Ltd; <https://www.alphawave.co.za/>) assuming continuous downlink 100% traffic loading, TDD operation and an antenna pattern based on the envelope of a single beam with maximum $EIRP_{max}$ along bore site of 73.2dBm. The algorithms implemented in the software are based on ray tracing techniques and use far field antenna pattern data as input to calculations to determine the free space fields in front of the antenna.

B. MEASUREMENTS AND DATA PROCESSING

EMF measurements were made using two NARDA SRM-3000 and five NARDA SRM-3006 meters connected to tri-axial isotropic E-field probes (75 MHz to 3 GHz or 420 MHz to 6 GHz) over a 1.5 or 5 m cable. Meters were configured to measure the time-averaged channel power in the 2.3 GHz band in consecutive 1-min periods which were later post-processed to produce 6-min sliding time-averaged values expressed as a percentage of the ICNIRP occupational reference level applicable for the frequency band used by the RBS (50 W/m²) [1]The position of the antennas and access restrictions at the site mean that ICNIRP occupational reference levels were the relevant limits. The 1-min samples were selected so that there was reasonable resolution in the data without creating data files too large to be stored

and manipulated. The resolution bandwidth was 3 MHz and sweep time 408 ms.

Measurements were conducted over four week days for a period of approximately eight hours per day, between 8 a.m. and 6 p.m. and each measurement was repeated for a second eight hour period hence 16 hours of measurements was gathered at each of the measurement locations.

III. RESULTS

A. MEASUREMENTS

The highest 6-min sliding average value for each probe position found over the 4-day measurement period, the computed theoretical maximum values (computational modelling) and the compliance boundary reduction factor (CBRF) are given in Table 1.

TABLE 1. Predicted and 6-min results expressed as % ICNIRP occupational reference level.

Probe location	Plane Hi			Plane Lo		
	Predicted	6-min	CBRF ^b	Predicted	6-min	CBRF ^b
1	73.7	2.5	5.4	72.5	2.5	5.4
2	80.4	3.7	4.7	78.4	3.2	4.9
3	85.4	4.0	4.6	82.1	4.3	4.4
4	84.4	5.4	4.0	80.1	4.1	4.4
5	79.3	7.3	3.3	79.2	4.9	4.0
6	77.8	4.1	4.4	76.6	na ^a	
7	76.7	3.4	4.7	75.2	2.4	5.6
Notes	na ^a = not available due to data logging fail Compliance boundary reduction factor (CBRF) ^b = (Predicted/6-min)					

The highest 6-min average value was 7.3% at location 5Hi adjacent to the nominal boresight position 4Hi while the predicted value at 5Hi including TDD reduction was 79.3%. The lowest 6-min values in plane Hi were 2.5% (1Hi) and 3.4% (7Hi) which is a reduction of 4.7 dB and 3.3 dB respectively relative to 5Hi. In plane Lo, the highest level recorded was 4.9% (5Lo) and the lowest levels were 2.5% (1Lo) and 2.4% (7Lo) which is a reduction of 2.9 dB and 3.1 dB respectively relative to 5Lo.

The CBRF is a measure of the overestimation of the size of the compliance boundary. It is defined as the square root of the ratio of the computed RF exposure to the 6-min average value and has a minimum value of 3.3 at location 5Hi. This suggests that the realistic compliance boundary is smaller by at least a factor of 3.3 times compared to the conservatively computed boundary.

In addition to EMF measurements, information was obtained from network counters that monitor the state of DL transmitter activity in the form of physical resource block (PRB) utilization. In LTE, no DL power control is used and power per PRB is constant. Therefore, the proportion of PRBs used, the PRB utilization, is proportional to the time-averaged transmitter power [5].

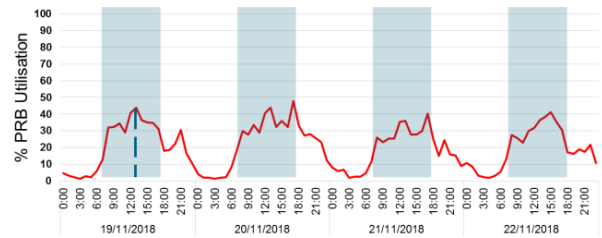


FIGURE 4. Percentage LTE physical resource block (PRB) over the four day measurement period starting Monday 19 November 2018. The highest 6-min value (7.3%) was found on the Monday at around 1.50 p.m. (dashed line). The light blue shaded regions represent the times during which EMF measurements were performed.

The plot in Fig. 4 is the time variation in PRB utilization over the four measurement periods. A 100% utilization equates to continuous DL transmitter operation. Utilization data shown here are hourly time-averaged values as 6-min time-averaged values were not available. The data shows that user traffic during the week day, between 8 a.m. and 6 p.m., generated 30% to 50% PRB utilization and reached maximum utilization during afternoons. At the highest 6-min value of 7.3%, PRB utilization reached 45% (Monday 19/11/2018, 1.50 p.m.).

An estimate of the 6-min average PRB utilization can be made by assuming that the hourly average value of 45% is either: a) representative of the 6-min value (similar traffic patterns) or; b) that the 6-min value may have reached 100% (period of high intensity traffic but not sustained over the full hour). This suggests that the 6-min average EMF values in Table 1 can be scaled by between 1 and 2.2 times to obtain estimates of exposure at 100% 6-min time-averaged PRB utilization. For example, exposure at 5Hi scaled to 100% utilization is between 7.3% and 16.1% of the limit value compared to a predicted, conservative level of 79.3%. This represents a far-field reduction in the occupational compliance boundary of between 2.2 and 3.3 times.

Plots in Fig. 5 are of the time aligned 6-min values from each of the seven probes in plane Hi for the period between 11.50 a.m. and 2.30 p.m. on the day of the highest recorded 6-min average value.

At around 9.15 a.m. the highest values were recorded by probes 2Hi and 6Hi indicating that EMF levels were momentarily higher away from bore site. Shortly after, probes 4Hi and 5Hi were higher while 2Hi and 6Hi were well down. At around 10.10 a.m. the highest values were those recorded by probes 3Hi, 4Hi and 5Hi with lower values recorded by probes 1Hi and 7Hi. This was immediately followed by 7Hi recording the highest EMF value. A similar picture emerges around 12.30 p.m. where probes 4Hi and 5Hi around bore-sight recorded the highest values however in the time that immediately followed, probe 6Hi recorded the highest value of any probe.

The highest 6-min average value of 7.3% was recorded by probe 5Hi at around 1.50 p.m. This short time sequence is indicative of how the radiation pattern of a mMIMO antenna

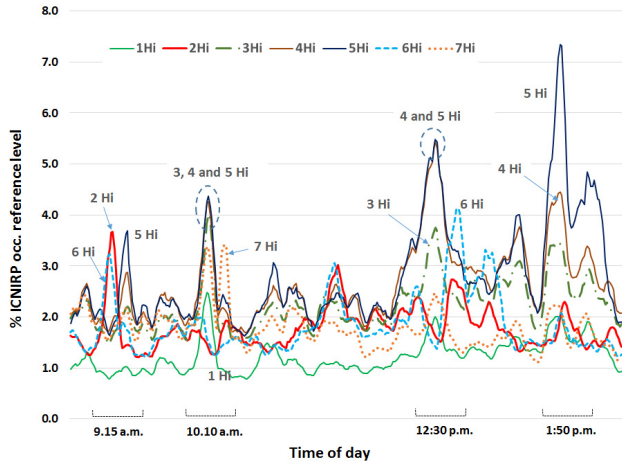


FIGURE 5. Time aligned 6-min sliding average values from individual probes in plane Hi expressed as a percentage of the ICNIRP occupational reference level measured on Monday 19 November 2018 from 11.50 a.m. to 2.30 p.m.

in a live network is dynamic and constantly changing rather than static as is the case for conventional sector antennas. The radiation pattern of the mMIMO antenna changes in response to the demands of users distributed spatially and temporally across the cell.

B. SUMMARY OF RESULTS

Measurements of EMF in front of the mMIMO antenna serving users in a dense urban environment indicate that when scaled to 100% PRB utilization the 6-min time-averaged RF exposure level was between 7.3% and 16.1% of the ICNIRP occupational reference level at 2.3 GHz. The conservative maximum computed RF exposure level (100% PRB utilization, TDD ratio 0.75) was 79.3% of the ICNIRP occupational reference level. The measured levels represent a far-field reduction in the occupational compliance boundary of between 2.2 and 3.3 times compared to computed values. A further reduction in the compliance boundary would occur if the actual maximum PRB utilization (e.g. 45%) is used as a proxy for maximum RBS power.

IV. OBSERVATIONS FROM EXAMPLE EXPOSURE SCENARIOS

The following example exposure scenarios were chosen to provide some insights into the behaviour of the time varying RF exposure observed during our measurement campaign.

In a mobile network, users may be stationary (office) or mobile (walking, in a car) and their data download relatively continuous (file download, movie streaming) or intermittent (browsing). The RBS scheduling protocol decides which subset of users should be served at any instant in time. In the following example exposure scenarios, it is not critical to know the details of the scheduling protocol or to assume particular user applications (e.g. web browsing, streaming video) but it is sufficient to assume that the system behaves

dynamically and ‘chaotically’, and that a stochastic approach to analysis is valid.

Consider the example cluttered environment shown in Fig. 6 as being representative of the dense urban environment in this study served by an RBS with a mMIMO antenna.

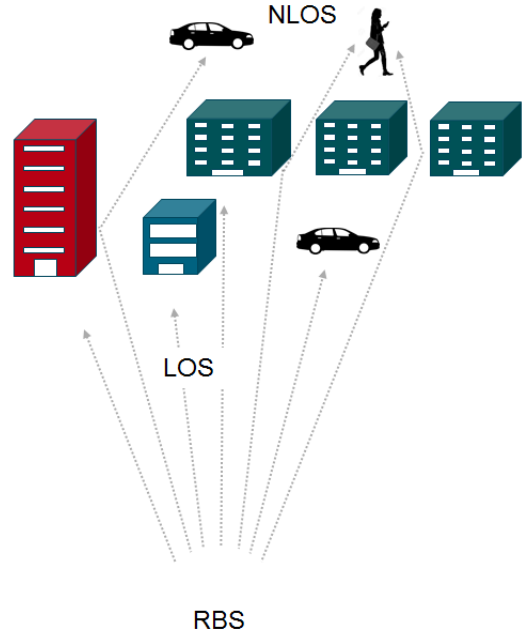


FIGURE 6. Simplified schematic showing the distribution of users served by a RBS with a mMIMO antenna. Propagation conditions create both LOS and NLOS connections.

The maximum EIRP of the RBS in this example is $EIRP_M$. In most measurement campaigns, it will not be possible to know the spatial distribution of users in a cell and how they are being scheduled by the RBS. Some users will be in line of sight (LOS), or partially in LOS of the RBS while others will be in non-LOS (NLOS) areas but still receiving service via scattered signals. These radio propagation environments are commonly referred to as Rician and Rayleigh fading respectively [10]. These propagation characteristics were evident at our measurement site shown in Fig.1 where many users were not in a clear, unobstructed LOS of the RBS. They were located either in buildings or relied on scattered signals for their connection to the RBS.

Scattering from objects in the environment is an important aspect of mMIMO networks since reflected signals can be usefully exploited as alternate, uncorrelated propagation paths that can improve transmission performance. User data can be split and sent simultaneously as multiple data streams over these paths using separate beams. Now we consider how this example scenario may influence EMF levels measured by probes at our measurement site under mMIMO beamforming operation.

In Fig. 7 we have superimposed a set of beams onto the cluttered environment shown in Fig. 6 along with seven EMF probes positioned in azimuth from φ_1 to φ_7 in front of the

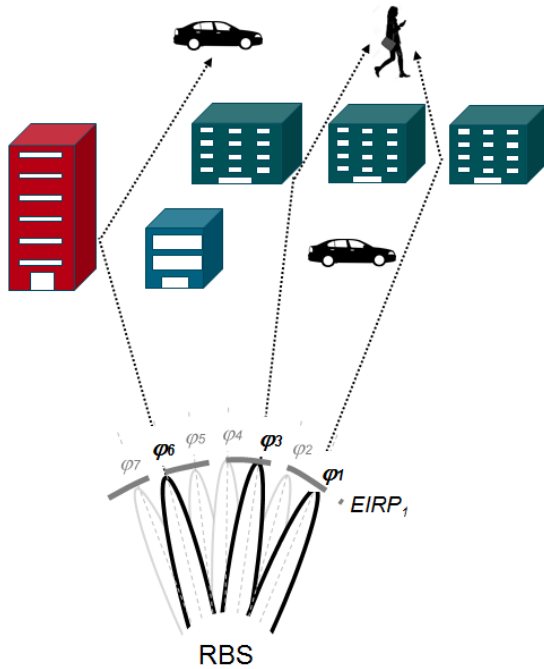


FIGURE 7. Simplified schematic at an instant in time t_1 showing active beams (bold lines) directed along φ_1 , φ_3 and φ_6 , each with $EIRP_1$.

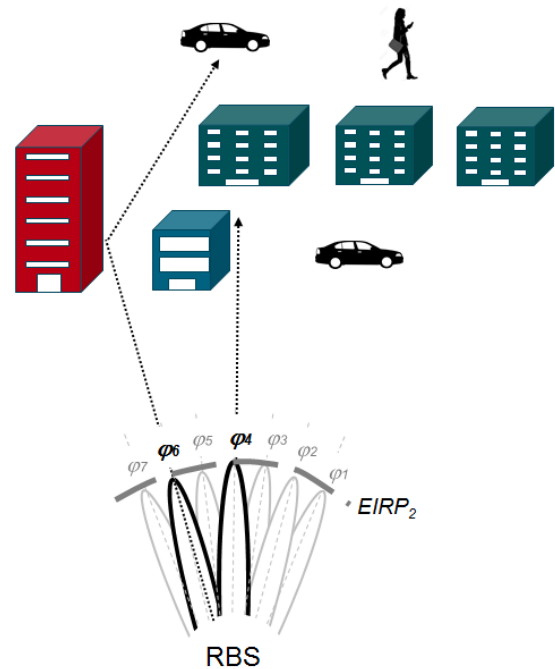


FIGURE 8. Simplified schematic at an instant in time t_2 showing active beams (bold lines) directed along φ_4 and φ_6 , each with $EIRP_2$.

mMIMO antenna (similar to that described in Section IIA but with elevation not considered).

At time instant t_1 a subset of users in NLOS areas are scheduled to be served simultaneously by 3 beams directed along φ_1 , φ_3 and φ_6 each with a radiated power $EIRP_1$ (equal to $EIRP_M - 10\log_{10}(3)$) which will be measured by the three EMF probes positioned along these three directions. The vehicle is served by the beam directed along φ_6 while the other user (walking) is served by two beams along φ_1 and φ_3 . Side lobe radiation from each active beam will simultaneously be present in all other directions contributing to the total EMF measured by each of the seven probes.

In Fig 8, in time instant t_2 , a subset of users are served by two beams simultaneously directed along φ_6 (serving the vehicle via a reflected path) and φ_4 (serving users in the building). The radiated power of the two beams is $EIRP_2$ (equal to $EIRP_M - 10\log_{10}(2)$) which will be measured by the two EMF probes positioned along φ_4 and φ_6 . As in Fig. 7, side lobe radiation from each active beam will simultaneously be present in all other directions contributing to the total EMF measured by each of the seven probes.

The following observations can be made about the examples in Figs 7 and 8. The time-averaged EMF levels (over t_1 and t_2) measured by probes at φ_2 , φ_5 and φ_7 are due to side lobe radiation only and will be well below levels in other azimuthal directions. The EMF levels measured at φ_1 , φ_3 and φ_4 are the average of radiation from scheduled beams and side lobe radiation. The average EMF level at φ_6 is due to scheduled beams at times t_1 and t_2 with contributions from side lobes at alternate times from beams φ_1 , φ_3 and φ_4 . The

radiated power of the scheduled beams changes between time instances. At t_1 the radiated power was $EIRP_1$ while at t_2 it was $EIRP_2$.

These examples illustrate some key behaviours of a mMIMO network and how they impact on measured EMF levels. The scheduling of beams can change with time and will in part depend on user demand for service and propagation conditions. These changes are dynamic and will influence the number of simultaneous beams scheduled in the service area. A statistically based theoretical study found that it was highly unlikely that all users would be concentrated within a single beam [6].

A second observation is that the angular direction of a scheduled beam is influenced not just by the spatial distribution of users (mobile or stationary) but also by scattering in the environment. This has the effect that users can appear to be spatially distributed over a large portion of the service area even if they are clustered over smaller areas. The EMF levels in Table 1 are highest near bore site and lower near the extreme azimuthal positions φ_1 and φ_7 which is consistent with the shape of the envelope of the radiation pattern of a mMIMO antenna. It is not however possible to infer from our measurements that users were uniformly spread throughout the service area only that the combination of users and the environment created an apparent uniform spread.

A third observation is that switching of beams in of itself creates a dynamic, time varying EMF environment that is influenced by user spatial positions, scattering from objects and RBS scheduling. Even if RBS traffic loading is constant at 100% utilization, the time varying direction and radiated

power of mMIMO beams means that EMF levels cannot be easily described deterministically, and it is often preferable to describe the field in terms of statistical parameters.

V. DISCUSSION

In this study, a series of measurements of the 6-min time-averaged EMF levels in front of a mMIMO antenna carrying live traffic in a dense commercial/industrial urban environment were compared with conservatively computed EMF levels at the same positions. The purpose of the comparison is to determine the extent of overestimation, if any, in the size of a conservatively computed EMF compliance boundary when compared to a boundary based on measured EMF levels from a mMIMO antenna operating in a live network. Furthermore, our observations in Section IV concerning RF exposures in a mMIMO network suggest that it may be preferable to describe EMF levels in terms of statistical parameters.

In [8] a study based on statistical modelling of the time-averaged EMF levels from 5G RBSs operating in TDD mode (ratio 0.75) using mMIMO antennas found that realistic levels (95th percentile) were about 15% of the theoretical maximum level (based on conservative assumptions) at a RBS utilization of 94% when users were uniformly spread in azimuth but no elevation scanning. The authors note that for far-field exposure, this equates to a reduction of the compliance boundary of about 2.6 times. Over a range of different user spatial distributions, the time-averaged realistic maximum (95th percentile) was 7% to 22% of the theoretical maximum - a reduction of the compliance boundary of between 3.8 and 2.1 times respectively.

In [9], a statistical approach was taken to compliance boundary assessments in mMIMO systems. It took into account 3GPP¹ channel models for realistic deployment scenarios in terms of installation height, user distribution and traffic found that at the 95th percentile for a TDD ratio of one (always transmitting), the actual time-averaged RBS power in an urban setting was 22% to 26% of the maximum transmit level when only one active user was considered. This results in a compliance boundary of around half that which would be calculated based on traditional conservative assumptions. The authors concluded that the RBS compliance boundary could be further reduced when a higher number of active users were served.

In this study the highest 6-min average EMF level scaled to 100% PRB utilization and for a TDD ratio of 0.75, was between 7.3% and 16.1% of the ICNIRP occupational reference level compared to a worst case predicted value of 79.3%. This represents a far field reduction in the compliance boundary of 2.2 to 3.3 times which is consistent with statistically based theoretical studies [8, 9]. Compliance approaches based on related actual maximum EIRP are also described in IEC 62269 [11].

Results of measurements presented in this paper and the observed reduction in the compliance boundary are expected

to be similar in 5G networks with mMIMO beamforming antennas. Future measurement studies should be conducted to explore compliance boundary reductions in other environments such as in residential/domestic settings, and to confirm that these findings apply to functioning 5G mMIMO networks.

VI. CONCLUSION

In this paper we found that the highest in situ measured EMF level from the 4G LTE TDD mMIMO antenna scaled to 100% PRB utilization was between 7.3% and 16.1% of the ICNIRP occupational reference level compared to 79.3% based on traditional conservative computational modelling. This represents a far field reduction in the conservatively computed compliance boundary of between 2.2 to 3.3 times, consistent with other statistically based theoretical studies. This reduction can be attributed to the intermittent, random like behavior of mMIMO beamforming. Additional studies are recommended to confirm that these findings apply to functioning 5G mMIMO networks and in other user environments such as in residential/domestic settings.

ACKNOWLEDGMENT

The authors acknowledge the very helpful technical assistance and access to equipment provided by Airmet Scientific Melbourne, Australian Radiation Protection and Nuclear Science Agency (ARPANSA), and Telstra Corporation Ltd. They also acknowledge the helpful comments and suggestions provided by Dr. J. Rowley, Dr. R. McIntosh, and Mr. M. Wood.

REFERENCES

- [1] The International Commission on Non-Ionizing Radiation Protection, "Guidelines for limiting exposure to time-varying electric, magnetic, and electromagnetic fields (up to 300 GHz)," *Health Phys.*, vol. 74, no. 4, pp. 494–522, Apr. 1998.
- [2] *IEEE Standard for Safety Levels with Respect to Human Exposure to Radio Frequency Electromagnetic Fields, 3 kHz to 300 GHz*, IEEE Standard C95.1-1991, Int. Committee Electromagn. Saf., New York, NY, USA, Apr. 2005.
- [3] *Determination of RF Field Strength, Power Density and SAR in the Vicinity of Radiocommunication Base Stations for the Purpose of Evaluating Human Exposure*, Standard IEC 62232:2017, Aug. 2017.
- [4] D. Colombi, B. Thors, T. Persson, N. Wirén, L.-E. Larsson, M. Jonsson, and C. Törnevik, "Downlink power distributions for 2G and 3G mobile communication networks," *Radiat. Protection Dosimetry*, vol. 157, no. 4, pp. 477–487, Dec. 2013.
- [5] D. Colombi, B. Thors, N. Wirén, L.-E. Larsson, and C. Törnevik, "Measurements of downlink power level distributions in LTE networks," in *Proc. Int. Conf. Electromagn. Adv. Appl. (ICEAA)*, Sep. 2013, pp. 98–101.
- [6] M. Wenhua, M. Huaxing, and G. Peng, "The EMF radiation calculation and measurement for smart antenna," in *Proc. 6th Int. Wireless Commun. Mobile Comput. Conf. (IWCMC)*, 2010, pp. 119–123.
- [7] S. Persia, C. Carciofi, S. D'Elia, and R. Suman, "EMF evaluations for future networks based on Massive MIMO," in *Proc. IEEE 29th Annu. Int. Symp. Pers., Indoor Mobile Radio Commun. (PIMRC)*, Bologna, Italy, Sep. 2018, pp. 9–12.
- [8] B. Thors, A. Furuskär, D. Colombi, and C. Törnevik, "Time-averaged realistic maximum power levels for the assessment of radio frequency exposure for 5G radio base stations using massive MIMO," *IEEE Access*, vol. 5, pp. 19711–19719, 2017.

¹3rd Generation Partnership Project (3GPP), <https://www.3gpp.org/>

- [9] P. Baracca, A. Weber, T. Wild, and C. Grangeat, "A statistical approach for RF exposure compliance boundary assessment in massive MIMO systems," in *Proc. Int. Workshop Smart Antennas (WSA)*, Bochum, Germany, Mar. 2018, pp. 1–6. [Online]. Available: <http://arxiv.org/abs/1801.08351>
- [10] F. Belloni. *Fading Models*. Accessed: Aug. 23, 2019. [Online]. Available: http://www.comlab.hut.fi/opetus/333/2004_2005_slides/Fading_models_text.pdf
- [11] *Case Studies Supporting IEC 62232—Determination of RF Field Strength, Power Density and SAR in the Vicinity of Radiocommunication Base Stations for the Purpose of Evaluating Human Exposure*, Standard IEC TR 62669:2019, Apr. 2019.



ROB WERNER received the associate Diploma degree in electronic engineering from the State Training Board of Victoria, in 1996. He was with Telstra in designing and commissioning radio systems and later in designing and optimizing mobile networks. In 2001, he moved overseas and managed the RF design of several mobile networks within Asia. Since 2008, he has been with Singtel Optus Pty Limited as a Senior Technical Specialist in EMF safety and compliance. He was a member of the Mobile Carriers Forum (MCF) Operations committee. He is currently a member of the Australian Mobile Telecommunications Association (AMTA) EMF Health and Safety committee and the GSMA EMF and Health committee.



PHILL KNIPE received the B.Sc., M.Phil., and Ph.D. degrees from Murdoch University, Australia, in 1990, 2002, and 2013, respectively, all in physics. Since 1991, he has been a Consultant Physicist in ionizing and non-ionizing radiation protection in Australia and internationally. In 2002, he set up Total Radiation Solutions Pty Ltd, which holds ISO 17025 and ISO 17020 accreditations. He is currently a member of Standards Australia Committee TE7 (EMF safety) and has been on the International Electrotechnical Commission (IEC) Group responsible for the development and maintenance of the IEC measurement and modeling of radio waves standard (62232), since 2007. He is currently an Affiliate Researcher with the Australian Centre for Electromagnetic Bioeffects Research (ACEBR). He has published in peer-reviewed journals in the measurement of electromagnetic fields. He is a committee member of the Australasian Radiation Protection Society (ARPS), and an executive and a joint member of the Bioelectromagnetics Society (BEMS) and European Bioelectromagnetics Association (EBEA).



STEVE ISKRA received the B.E. degree (Hons.) in electrical engineering from the University of Melbourne, Australia, in 1982, and the Ph.D. degree from RMIT University, in 2012. Since 1982, he has been with Telstra Corporation Ltd., where he was involved in the fields of EMC and EMF safety. He has published in peer-reviewed journals in the areas of EMC, human exposure to electromagnetic fields, and RF personal dosimetry. He was a Chairman of the Standards Australia Committee TE/3 (EMC) and is currently a Member of the Standards Australia Committee TE/7 (EMF safety). In 2004, he received a Standards Australia Award for outstanding service to the national and international work of Committee TE/3. He is currently an Associate Investigator with the Australian Centre for Electromagnetic Bioeffects Research (ACEBR), an Adjunct Research Fellow with Swinburne University of Technology, and a Member of the Bioelectromagnetics Society (BEMS).

• • •